Ductile High-Tg Epoxy Systems via Incorporation of Partially Reacted Substructures

Journal:	*Journal of Materials Chemistry A*
Manuscript ID	TA-ART-08-2020-008158.R1
Article Type:	Paper
Date Submitted by the Author:	02-Nov-2020
Complete List of Authors:	Sharifi, Majid; Drexel University, Chemical and Biological Engineering Palmese, Giuseppe; Drexel University, Chemical and Biological Engineering

SCHOLARONE™
Manuscripts

ARTICLE

Ductile High-T$_g$ Epoxy Systems via Incorporation of Partially Reacted Substructures

M. Sharifi[a] and G. R. Palmese[a]

A method is demonstarted for obtaining high glass transition temperature (T$_g$) plastically deformable crosslinked polymer systems by manipulating network topology of epoxy systems cured with amines. Long-chain Monoamine-functionalized Partially Reacted Substructures (mPRS) were synthesized by reacting a mixture of tetraglycidyl ether of diaminodiphenylmethane (TGDDM) and polyether monoamine (PEMA) to varying extents. Predetermined amounts of the mPRS having 0%, 60%, and 80% degree of polymerization were added to a mixture of a TGDDM and polyether diamine (PEDA) as well as a mixture of diglycidyl ether of bisphenol-A (DGEBA) and PEDA. Results of quasi-static tensile tests performed on the cured samples reveal pronounced strain hardening and, subsequent, large elongation-to-failure in the modified epoxy systems containing mPRS with elevated degrees of polymerization. Thus materials with distinctly improved elongation-to-failure are obtained for systems with identical overall chemical composition. The striking difference is attributed to plastic microvoid growth aided by the presence of deformable mPRS domains. Fracture surfaces of deformed mPRS modified systems show the characteristic formation of microvoids. In comparison, similar systems based on less deformable diamine functionalized substructures (PRS), on which we reported prviously, did not show the same propensity to yield and deform plastically.

Introduction

Epoxy thermosets are among the most important polymeric materials, as they are widely used in the manufacturing processes of composites, structural materials, adhesives, and coatings. A highly crosslinked structure of an epoxy polymer generally provides good-to-excellent mechanical properties, however, it makes the epoxy polymer brittle. As a result, numerous studies have been focused on improving the brittleness of highly crosslinked epoxy polymers without affecting other advantageous physical and mechanical properties such as strength, elasticity, and glass transition temperature.

Accordingly, one aspect of these studies has been focused on toughening epoxy systems by incorporating soft particles such as rubber particles,[1-3] multi-block copolymers,[4-7] interpenetrating polymer networks,[8, 9] elastomers,[10-12] and thermoplastic phases[13, 14] into the crosslinked structure of epoxy systems. In addition, the incorporation of functionalized soft particles was shown to be effective at improving the toughness of these epoxy systems.[15, 16] However, the presence of soft particles in a polymer network (e.g., an epoxy system) generally degrades advantageous mechanical properties, particularly mechanical strength and elasticity. To overcome this issue, a number of researchers discovered the effectiveness of incorporating core/shell particles into toughening epoxy systems with minimal reduction in mechanical properties.[17-19]

In another study, toughened epoxy systems were achieved by incorporating rigid particles, for example, adding ceramic nanoparticles such as silica,[20-22] titanium oxide,[23] zinc oxide,[24] iron oxide,[25] tungsten disulphide,[26] alumina,[27] graphene platelets,[28] carbon nanotubes,[29] fullerene,[30] and so forth. In some other studies, it was revealed that incorporating functionalized rigid particles was also beneficial toward toughening epoxy systems.[31] For example, properties of an epoxy system can be tailored via the use of amine-functionalized polyhedral oligomeric silsesquioxane (POSS).[32]

Recently, a series of coarse-grained molecular simulations suggested that a void-growth mechanism in a highly crosslinked polymer considerably enhances the ductility of the polymer without affecting the tensile strength and the Young's modulus.[33, 34] This mechanism of void growth is based on the presence molecular surfaces that are not covalently bound and can open when strained to form voids without breaking chemical bonds. These features in the network topology (connectivity of the cross-link junctions throughout the network) were termed protovoids. Based on these simulation studies, a processing method was proposed and investigated that used a solvent to enhance and control the creation of unbound molecular surfaces within a highly crosslinked epoxy system.[35] In this method, a network is created in the presence of the solvent that is then removed creating protovoids in proportion to the amount of solvent used. It was shown that upon tensile loading, the epoxy system exhibits greatly increased plastic deformation, without the T$_g$,tensile strength, density, and the Young's modulus, being significantly affected. The results of this experimental study was further supported by a series of atomistic molecular simulations.[36]

The method of processing the epoxy systems as studied by Sharifi et al.[35], however, was not applicable to high-T$_g$ epoxy

a. Department of Chemical and Biological Engineering, Drexel University, 3141 Chestnut Street, Philadelphia, Pennsylvania 19104, United States.

This journal is © The Royal Society of Chemistry 2020

J. Mater. Chem. A., 2020, **00**, 1-3 | **1**

systems as the method uses an organic solvent to create the imbedded molecular surfaces, and thus a complete removal of the organic solvent in high-T_g epoxy systems is not achievable. Furthermore, this method is practical only for thin layers like coating for which the time for diffusion of the solvent from the network is short and the volume change is not problematic. Therefore, in a separate study, a new processing method was introduced as an attempt to imbed molecular surfaces in the crosslinked structure of an epoxy system by using partially reacted substructures designed to localize long chain diamines (PRS) to produce proptovoids.[37] This introduced a solventless topology-based method to toughen high-T_g epoxy systems without affecting advantageous mechanical (e.g., tensile strength, Young's modulus, etc.) and thermal properties (e.g., glass transition temperature, etc.).

Although a toughened epoxy was successfully produced by this processing method (using partially reacted substructures), the network's structure was not consistent with the structure that was envisioned in the simulations [33, 34, 36] or the structures obtained by initial investigations designed to produce protovoids[35]because the PRS substructures were bound too tightly to the rest of the network .[35] Accordingly, an important modification of the solventless processing methodology, based on our previous study[37], is proposed, wherein partially reacted substructures are produced from monoamine molecules. In this study, these substructures are referred to as "monoamine-functionalized partially reacted substructures" (or mPRS). The advantage of using monoamine molecules in the composition of partially reacted substructures is that the monoamines bond to the mPRS from one side while the other side freely stays inside a polymer network. In this work we show that the mechanical performance of the epoxy systems reinforced with mPRS is consistent with what was observed by the molecular simulation studies.[33, 34] In addition, the proposed method can be applied to high-T_g epoxy systems, as it does not require the use of an organic solvent to create imbedded molecular surfaces that are not covalently bound.

Experimental

Materials. Tetraglycidyl of diaminodiphenylmethane (i.e., TGDDM) provided by Sigma-Aldrich was used as the epoxy resins. Additionally, a polyether monoamine, also referred to as "PEMA", (i.e., Jeffamine M-1000® provided by Huntsman) was used as the monoamine to formulate an mPRS resin. The PEMA is predominately polyethylene glycol (PEG) based with a propylene oxide (PO) to ethylene oxide (EO) molar ratio of about 3:19. Moreover, a polyether diamine, also referred to as "PEDA", (i.e., Jeffamine D230® provided by Huntsman) was used as the primary curing agent (i.e., the curing agent of the dominant epoxy phase, not the mPRS phase). The molecular structures of these materials are shown in Figure 1.
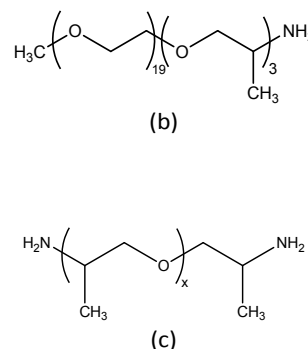

(a)

(b)

(c)
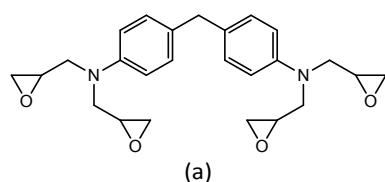
Figure 1. Chemical structure of each component used in this study: (a) tetraglycidyl of diaminodiphenylmethane (TGDDM), (b) polyether monoamine (PEMA), MW~= 1000 g/mol, PO:EO = 3:19 , (c) polyether diamine (PEDA), MW~= 230 g/mol, x~2.5.

Polymer processing. Polymeric samples in this study were prepared via using the following procedure: (1) preparing the monoamine functionalized Partially Reacted Substructures (or the mPRS resins) with controlled degree of polymerization; (2) preparing stoichiometric blends of blank samples of TGDDM and PEDA; (3) preparing sample mixtures by adding predetermined amounts of the mPRS resins to the blank samples (i.e., TGDDM + PEDA + mPRS); and (4) curing the sample mixtures.

Preparation of the mPRS resins. According to the first step of the processing method given above, a stoichiometric mixture of TGDDM (component (a) in Figure 1) and PEMA (component (b) in Figure 1) was prepared by adding PEMA to TGDDM with a molar ratio of 2:1 (i.e., two moles of PEMA per each mole of TGDDM). It should be noted that both PEMA and TGDDM were very viscous at room temperature, and thus a predetermined amount of each component was individually heated up to 110 °C and further kept isothermal for less than 5 minutes at that temperature prior to mixing. The preheated PEMA and TGDDM were then mixed in a preheated vial and well stirred at some elevated temperatures (e.g., 80 °C) for at least five minutes, or until a transparent looking mixture (i.e., an mPRS mixture) was obtained. The mPRS mixture was further oven-cured at 80 °C until a desired degree of polymerization was achieved.

Fourier Transform Infrared Spectroscopy (FTIR). The degree of polymerization of the mPRS mixture was measured by a Nexus 870 FTIR spectrometer (Thermo Nicolet Corp.) in the near-IR region. Figure 2 represents the FTIR spectra of the mPRS mixture over a period of 20 hours. The peaks at around 4530 cm^{-1} relate to a combination of stretching and bending of oxirane bands, whereas the peaks at around 6080 cm^{-1} relate to the first overtone of stretching vibrations of oxirane bands.[38] The disappearance of both peaks indicates the concentration of oxirane (or epoxide) groups in the mPRS mixture is reduced over time. On the other hand, the peak at around 4930 cm^{-1} relates to a combination of stretching and bending of primary amine bands, whereas the peak at around 6570 cm^{-1} relates to a symmetric stretching vibration of primary amine bands.[38] Accordingly, the peak at 4930 cm^{-1} correlates with the instantaneous concentration of the primary amine, whereas the

peak at 6570 cm^{-1} correlates with the instantaneous concentration of both the primary and secondary amine present in the mPRS mixture. Similarly, the disappearance of these peaks also indicates the amine (i.e., the primary and the secondary amine) concentration in the mPRS mixture is reduced over time. The reduced concentration of the primary amine, the

secondary amine, and the oxirane groups in the mPRS mixture, and also the formation of hydroxyl groups (indicated by the appearance of the peak at around 7000 cm^{-1}, which relates to the stretching vibrations of hydroxyl groups in the mPRS mixture) indicates an epoxy-amine reaction took place in the mPRS mixture.
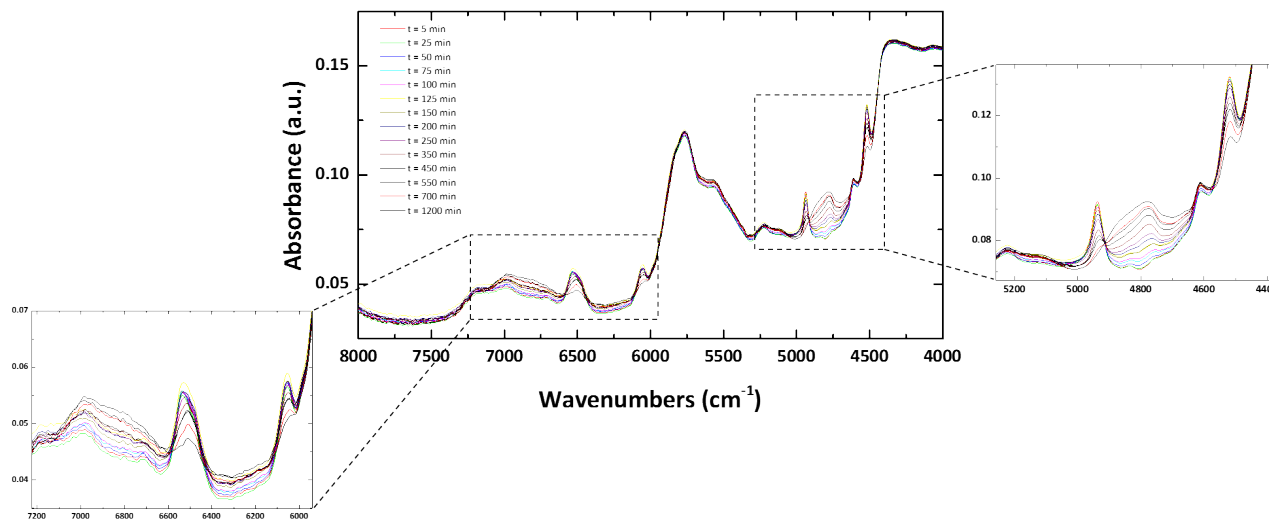

Figure 2. FTIR spectra (at near-IR region) of an mPRS mixture at 80 °C over a period of 20 hours.

Figure 3 shows the degree of polymerization of the mPRS mixture, which was measured with respect to the consumption of the oxirane groups present in the mPRS mixture relative to the initial concentration of the oxirane groups. Based on these results, the mPRS mixtures were reacted in an oven at 80 °C for approximately 16 hours and 35 hours to obtain 60%-converted and 80%-converted mPRS resins, respectively. The unreacted mPRS mixture is referred to as 0%-converted mPRS resin. Once a desired degree of polymerization was reached, the mPRS resins were immediately cooled to room temperature to quench the epoxy-amine reactions and to ensure reactions do not advance beyond the specified degrees of polymerization. Under these conditions, the mPRS resins are still reactive towards components of the blank mixture (i.e. TGDDM and PEDA), and will be covalently bond to the blank mixture during curing of the whole mixture.. The resulting mPRS resins were labelled 0%, 60%, and 80% conversion mPRS resins. It should be noted that the mPRS resins were crystallized when cooled to a sub-ambient temperature with a melting point around 26 °C. This is an advantageous property, particularly from shelf life perspectives, because curing reactions are extremely slow when the resin is present in a crystal form. Also, glass transition temperature of a fully reacted mPRS resin was found to be around -58 °C
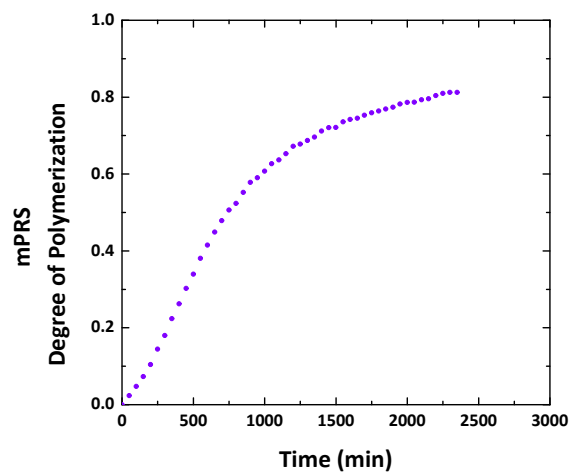

Figure 3. Degree of polymerization of the mPRS mixture. Reaction temperature was held at 80 °C.

Processing the blank, the mPRS-control, and the mPRS-modified samples. A predetermined amount from each of the resulting mPRS resins (i.e., 0%, 60%, and 80% conversion mPRS resins) was added to the blank samples (i.e., the stoichiometric blends of TGDDM and PEDA) to form sample mixtures having 10wt% and 20wt% mPRS resin, respectively. The resulting sample mixtures were well mixed and degassed with a centrifugal mixer, then oven-cured at 80 °C for 24 hours, and further post-cured at 160 °C for 4 hours. The resulting cured samples were categorized with respect to the degree of polymerization of the included mPRS resins. Accordingly, those cured samples that include 0%-converted mPRS resins were labelled "mPRS-

This journal is © The Royal Society of Chemistry 2020

J. Mater. Chem. A., 2020, **00**, 1-3 | **3**

control", whereas the ones that include 60%-converted and 80%-converted mPRS resins were labelled "mPRS-modified".

To further clarify, cured samples having the same composition and different mPRS degree of polymerization were considered "system isomers" because while they possess the same overall chemical composition, they vary in molecular arrangement of network building blocks due to variations in the mPRS degree of polymerization. For example, mPRS-control, 60%-converted mPRS-modified, and 80%-converted mPRS-modified samples having 10wt% mPRS resin (of 0%, 60%, and 80% conversion mPRS resins, respectively) are system isomers. In addition to the mPRS-control and the mPRS-modified samples, a set of blank samples (i.e., the stoichiometric blends of TGDDM and PEDA) were also prepared using the same curing protocol as in the mPRS-modified and the mPRS-control samples.

No macroscopic phase separation was observed for any of the above-mentioned formulations during mixing, curing, and post-curing. This observation suggests that PEMA is homogenously dissolved with TGDDM and PEDA in the sample mixture of the mPRS-control, and remains miscible during the cure/post-cure. Similarly, it suggests that the mPRS resin is homogenously dissolved with TGDDM and PEDA in the sample mixture of the mPRS-modified, and remains miscible during the cure/post-cure.

It is important to cure all the sample mixtures using the same curing protocol. If sample mixtures had been cured at different reaction temperatures, further observations of different thermal and mechanical properties of the cured samples may not solely relate to the presence of the mPRS resin or the degree of polymerization of the mPRS resin. It was shown that a difference in the curing temperature of an epoxy-amine reaction system results in a difference in the substitution factor (i.e., k_2/k_1) of the epoxy-amine reactions.[39] The difference in the substitution factor may form polymer networks with different network topologies, and thus epoxy systems that have experienced different reaction temperatures can yield different system isomers.

Dynamic Mechanical Analysis (DMA). Glass transition temperature of each cured sample was measured using a TA-Q800 dynamic mechanical analyzer in the single cantilever mode. Accordingly, rectangular specimens with a length of about 34–36 mm, a width of about 10–12 mm, and a thickness of about 2 mm were carefully cut. The specimens were heated at a temperature ramp rate of 2 °C/min under a cyclic displacement with a frequency of 1 Hz and an amplitude of 15 μm.

Mechanical testing. Two sets of experiments were conducted in this study: i) quasi-static tension, in view of ASTM D638, to evaluate quasi-static tensile properties of the cured samples; ii) compact tension, in view of ASTM D5045, to determine strain energy release rate (G_{1c}) of the cured samples. For the quasi-static tension test, at least six dog-bone shape specimens were precisely cut. Each specimen had an average thickness of about 2 mm, an average width of about 4 mm, and a gauge length of about 25 mm. The specimens were strained under a uniaxial tensile load provided by a servo-hydraulic INSTRON apparatus at a crosshead speed of 1 mm/min. For the compact tension

test, at least eight compact tension specimens were prepared from each cured sample. A fresh razor blade was used to induce a sharp crack prior to loading. The specimens were loaded at a crosshead speed of 1 mm/min using the servo-hydraulic INSTRON apparatus.

Scanning Electron Microscopy (SEM). A Zeiss Supra 50VP with an in-lens imaging detector was used to take high-resolution micrographs. Each specimen was first broken, and fracture surfaces were subsequently platinum-sputtered for 25 seconds prior to imaging.

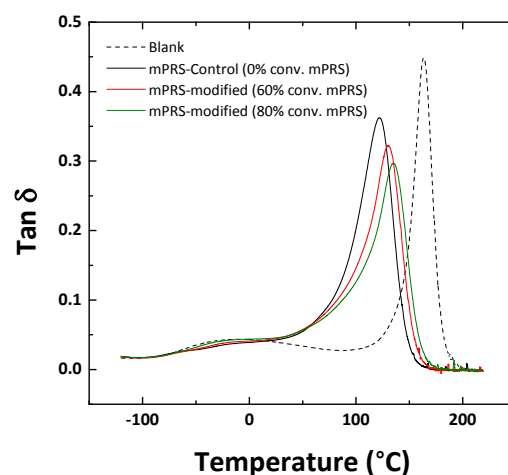## Results and Discussion

Figure 4. Tan δ of the blank, the mPRS-control, and the mPRS-modified systems having 20wt% mPRS resin.
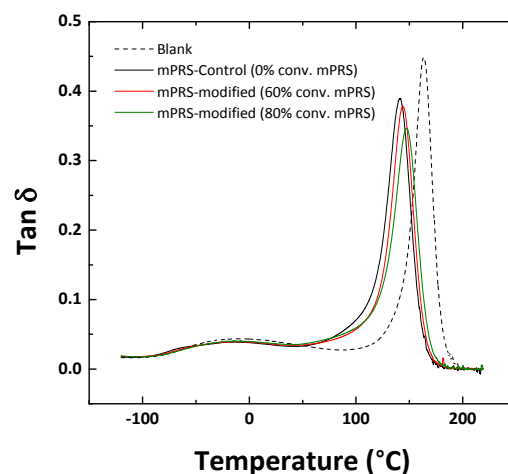

Figure 5. Tan δ of the blank, the mPRS-control, and the mPRS-modified systems having 10wt% mPRS resin.

Glass transition temperature. Figures 4 and 5 show the tan δ vs. temperature curves of the blank, the mPRS-control, and the mPRS-modified samples at 10wt% and 20wt% mPRS inclusion, respectively. T_g values for all specimens were measured based on the peak

4 | *J. Mater. Chem. A.*, 2020, **00**, 1-3

This journal is © The Royal Society of Chemistry 2020

position of the tan δ vs. temperature curves and are listed in Table 1. The T_g of the mPRS-modified systems correlates with the degree of polymerization of the mPRS resin used. This behavior was observed previously,[37] wherein different types of partially reacted substructures were incorporated into the crosslinked structure of an epoxy system comprising DGEBA and diethyltoluenediamine. In that study, it was discussed that the PRS-modified systems generally reveal higher T_g's than the corresponding control systems, and this observation was attributed to the way toughening agents disperse within the epoxy system. This observation has also been predicted by an atomistic molecular simulation elsewhere.[40] Likewise, in the structure of the mPRS-control samples, each PEMA molecule is likely surrounded by an epoxy (i.e., TGDDM) and an amine (i.e., PEDA); however, in the structure of the mPRS-modified samples, each PEMA molecule is likely confined by other PEMA molecules, as they are aggregated in mPRS regions. Since PEMA has a flexible backbone, it likely enhances the mobility of its neighbors within the structure. Therefore, the average fluctuation of epoxies and amines of the mPRS-control samples is slightly higher than that of the average fluctuation of epoxies and amines of the mPRS-modified samples at a given constant temperature. As a result, at the same overall composition, the T_g of the mPRS-modified systems is slightly higher (about 10–15 °C) than that of the mPRS-control systems. The trend of T_g increasing with the increasing degree of polymerization of the mPRS in the mPRS-modified systems can also be explained accordingly.

Quasi-static tensile properties. In the previous experimental and molecular simulation studies, it was shown that the presence of the "molecular surfaces" significantly improves the ductility of a highly crosslinked epoxy in glassy state.[33-36] On the other hand, incorporating the mPRS resins in the crosslinked structure of a polymer network could produce molecular surfaces as those shown in Figure 6. As a result, the mPRS-modified systems are expected to represent a similar strain hardening behavior as observed in the work of Mukherji et al.[33, 34] and Sharifi et al.[35]
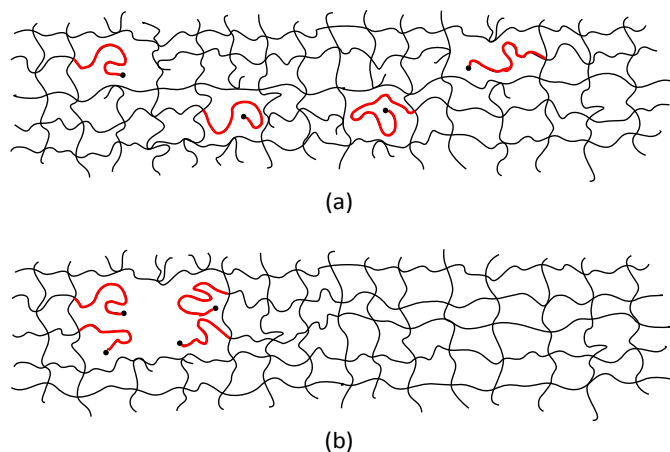

(a)

(b)

Figure 6. Polymer network structure of (a) an mPRS-control system, and (b) an mPRS-modified system at the same overall composition.

In the previous experimental study[35], a large plastic deformation was observed in a crosslinked epoxy system with a glass transition temperature of about 60 °C. The proposed

processing method of that experimental study was not applicable to epoxy systems with a T_g of above 100 °C due to the presence of a volatile sacrificial solvent. However, this study is applicable to any epoxy system (and perhaps any crosslinked thermoset) since the processing method does not rely on a sacrificial solvent; further, the mPRS resin can be incorporated into any epoxy system, as long as macro-phase separation does not occur.

To investigate the quasi-static tensile behavior of the cured samples, at least six dog-bone shape specimens of each blank, mPRS-control, and mPRS-modified samples were prepared. Each specimen had an average thickness of about 2 mm, an average width of about 4 mm, and a gauge length of about 25 mm. The specimens were strained under a uniaxial tensile load provided by a servo-hydraulic INSTRON apparatus at a crosshead speed of 1 mm/min.

Figure 7 shows the representative tensile stress-strain behavior of the system isomers (i.e., the mPRS-control and the mPRS-modified systems) reinforced with 20wt% mPRS resin. As shown in Figure 7, both the 60%-converted and the 80%-converted mPRS-modified systems revealed much larger elongation-to-failure than that of the mPRS-control systems. This promising improvement in tensile performance of the mPRS-modified is obtained with a slight drop in Young's modulus and tensile strength.
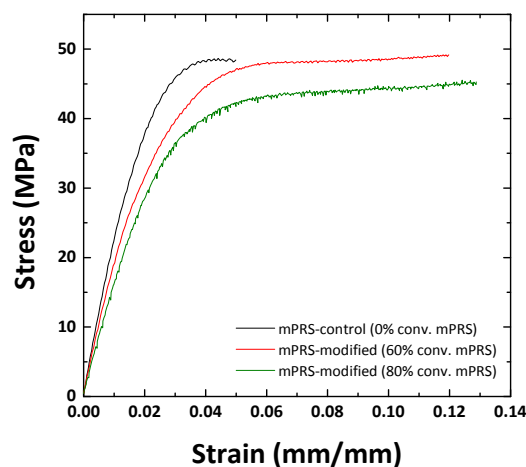

Figure 7. Representative stress-strain curves of the mPRS-control and the mPRS-modified systems having 20wt% mPRS resin.

As discussed previously, one thought is that the inclusion of the molecular surfaces in the crosslinked structure of the mPRS-modified systems boosted the values of elongation-to-failure by more than a 100% increase without substantially reducing Young's modulus, tensile strength, and T_g when compared to that of the mPRS-control systems. The remarkable elongation-to-failure of the mPRS-modified systems originates from greater energy absorbing mechanisms (i.e., localized shear deformation and plastic microvoid growth) without bond breaking. In fact, plastic microvoid growth is considerably enhanced in the mPRS-modified systems due to the presence of the molecular surfaces, and thus the contribution of the plastic microvoid growth to the total energy absorbed by the mPRS-

modified systems is much larger than that of the mPRS-control systems. Evidence of the plastic microvoid growth was captured in the micrographs of the fracture surfaces of the mPRS-modified systems, as shown in Figure 8.
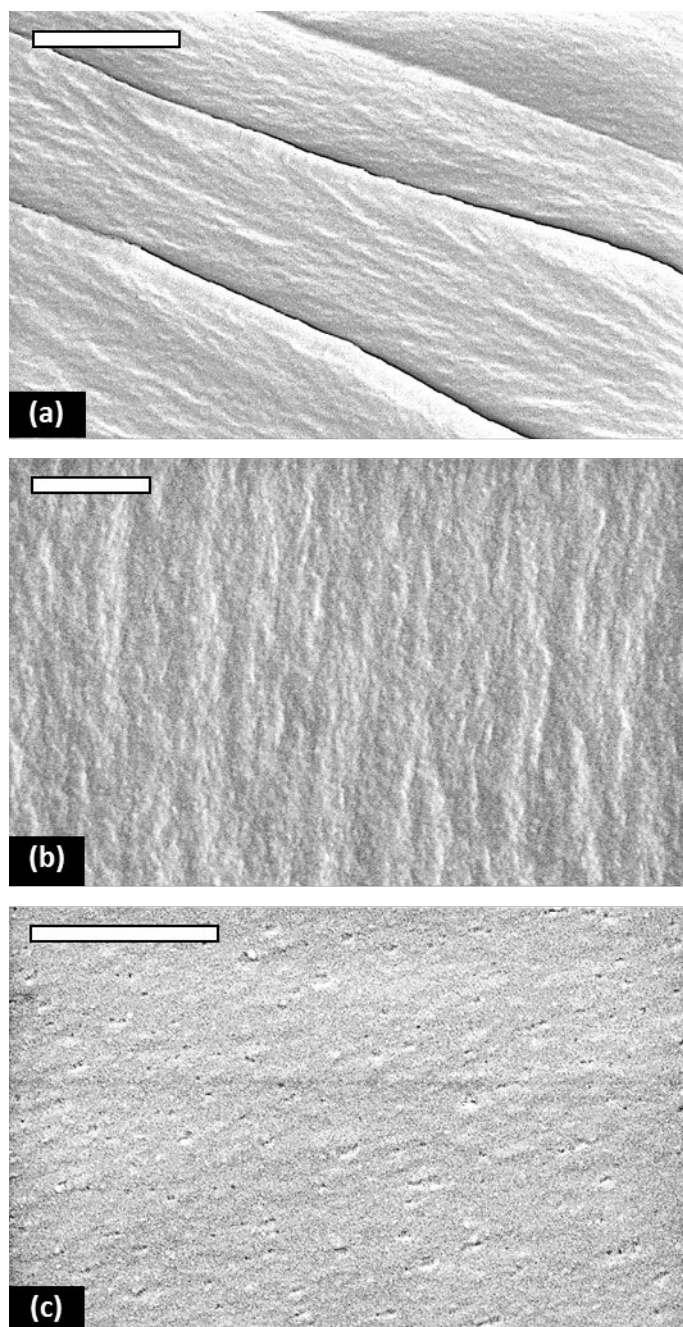

Figure 8. Representative SEM micrographs from the fracture surfaces of the a) blank, b) mPRS-control, and c) mPRS-modified systems (80% conv.) having 10wt% mPRS resin. Scale bars are 1 µm.

Additionally, Figures 9 and 10 show the representative tensile stress-strain behavior of the mPRS-control and the mPRS-modified systems at different mPRS inclusions. As expected, increasing the mPRS inclusion reduces the Young's modulus and the tensile strength in both the mPRS-control and the mPRS-modified systems; however, the large elongation-to-failure, as

observed in the mPRS-modified systems, has never been observed in the controls.
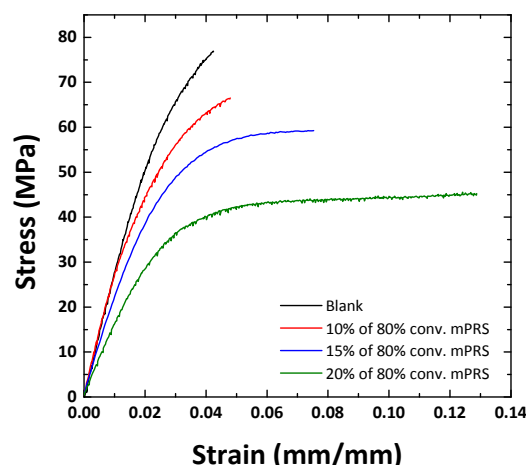

Figure 9. Representative tensile stress-strain curves for the mPRS-modified systems having 0wt%, 10wt%, 15wt%, and 20wt% mPRS resin (all having 80%-converted mPRS).
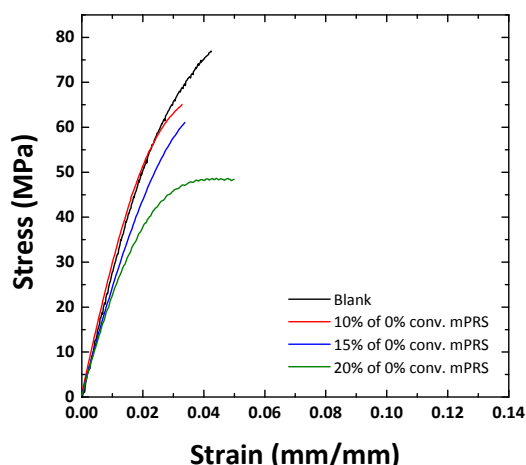

Figure 10. Representative tensile stress-strain curves for the mPRS-control systems having 0wt%, 10wt%, 15wt%, and 20wt% mPRS resin (all having 0%-converted mPRS).

The average values of Young's modulus, tensile strength, and elongation-to-failure of each blank, mPRS-control, and mPRS-modified system at different mPRS inclusions and different mPRS degree of polymerization are listed in Table 1. The average values of each data-point and the associated deviations were obtained from at least six replicates.

Similar experiments were carried out on mPRS-control and mPRS-modified systems, wherein the mPRS is made of monoamine molecules with a smaller molecular weight of about 600 g/mol. The results indicated the large elongation-to-failure—as observed in the mPRS-modified systems reinforced with 1000 g/mol PEMA—was not observed in the mPRS-modified systems reinforced with 600 g/mol PEMA. In fact, the difference between the mPRS-control and the mPRS-modified systems reinforced with 600 g/mol PEMA was insignificant. The lack of large elongation-to-failure in the mPRS-modified

6 | *J. Mater. Chem. A*, 2020, **00**, 1-3

This journal is © The Royal Society of Chemistry 2020

ARTICLE

systems reinforced with 600 g/mol PEMA could be due to relatively indistinguishable network topologies between system isomers (i.e., the mPRS-control and the mPRS-modified systems). Furthermore, when smaller PEMA molecules (and subsequently smaller mPRS) are used, the mPRS-control systems' network topology tends to look more like the network topology of the mPRS-modified systems. In contrast, the mPRS-modified systems' larger PEMA molecules (and subsequently larger mPRS) differentiate the network topology of the mPRS-modified systems from that of the mPRS-control systems.

Fracture toughness. In addition to the quasi-static tensile test, facture behavior of the blank, mPRS-control, and mPRS-modified systems were investigated via a compact tension te**st.**Values of the strain energy release rate (i.e.,G_{1c}) of each blank,

mPRS-control, and mPRS-modified systems at 10wt% and 20wt% mPRS inclusions were measured. The average values of each data set and the corresponding standard deviations, are listed in Table 1.

Fracture behavior of the mPRS-control and the mPRS-modified systems were consistent with our earlier findings.[37] In our previous study, the toughness improvement of a PRS-modified system was suggested to be due to the presence of low-T_g nanostructures that are dispersed within the modified epoxy systems. In this study, similar low-T_g nanostructures (in the form of mPRS regions) are also dispersed within the mPRS-modified systems of this study. Figure 11 illustrates the difference between the network structure of an mPRS-modified system (of this study) and a PRS-modified system (of our previous study).
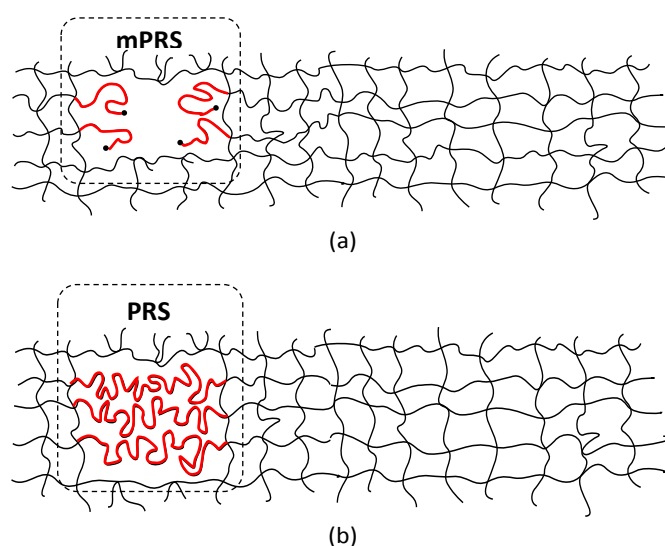

(a)

(b)

Figure 11. Polymer network structure of (a) an mPRS-modified system and (b) a PRS-modified system.[37]

Table 1. Average values of Young's modulus, tensile strength, elongation-to-failure, glass transition temperature, and strain energy release rate of the blank, mPRS-control, and mPRS-modified systems.

		Young's modulus (GPa)			Tensile strength (MPa)			Elongation-to-failure (%)			T_g (°C)			G_{1c} (J/m²)		
		mPRS degree of polymerization			mPRS degree of polymerization			mPRS degree of polymerization			mPRS degree of polymerization			mPRS degree of polymerization		
		0%	60%	80%	0%	60%	80%	0%	60%	80%	0%	60%	80%	0%	60%	80%
mPRS Inclusion	0%	2.7 ± 0.1			73.7 ± 6.6			4.5 ± 0.3			163			157 ± 12		
	10%	2.8 ± 0.1	2.5 ± 0.1	2.6 ± 0.2	61.7 ± 6.6	66.2 ± 2.5	63.5 ± 2.4	3.3 ± 0.9	5.3 ± 0.8	4.6 ± 0.3	141	144	148	220 ± 94	474 ± 88	508 ± 166
	15%	2.4 ± 0.1	N/A	2.1 ± 0.1	61.1 ± 3.4	N/A	58.9 ± 2.3	3.4 ± 1.3	N/A	7.3 ± 2.2	134	N/A	149	N/A	N/A	N/A
	20%	2.0 ± 0.2	1.8 ± 0.1	1.6 ± 0.1	47.9 ± 0.6	48.4 ± 0.8	45.1 ± 0.6	5.4 ± 1.9	9.7 ± 1.6	8.9 ± 2.7	121	130	135	319 ± 136	348 ± 96	343 ± 53

In the mPRS-modified systems of this study, the presence of the low-T_g nanostructures (indicated as "mPRS" in Figure 11-a) enhances the energy absorbing mechanisms that occur in highly crosslinked thermosetting systems, such as localized shear

deformation and plastic void-growth. In fact, plastic void-growth seems to occur within the low-T_g nanostructures (i.e., the mPRS regions) as shown by the evidence of void opening that appeared on the fracture surfaces of the mPRS-modified

systems, shown in Figure 8-c. The enhanced plastic void-growth delays the covalent bond breaking and crack initiation, thereby causing the fractures to form at larger strains. As a result, the mPRS-modified systems revealed a relatively larger (G_{1c}) than that of the mPRS-control systems at the same overall composition. This phenomenon is similar to what was observed in the PRS-modified systems.[37]

Application of the mPRS-toughening to a DGEBA-based epoxy system. So far, the results have indicated the effectiveness of using the mPRS resins to improve the ductility and the toughness of an amine-cured epoxy system comprising tetraglycidyl of diaminodiphenylmethane (TGDDM) cured with polyether diamine (PEDA, MW~=230 g/mol). Since the proposed toughening was shown to be a topology-based toughening (i.e., only relating to a polymer's network topology and not to the composition of the polymer network), it may be applicable to other thermosetting systems that form a crosslinked network structure. One example of a widely used epoxy resin is diglycidyl ether of bisphenol-A (DGEBA). In a separate investigation, the mPRS-toughening method, as described, was applied to an amine-cured epoxy system composed of DGEBA (i.e., EPON-825) provided by Miller-Stephensen and polyether diamine (PEDA, MW = 230 g/mol) provided by Huntsman.

The method of producing the mPRS resin was substantially similar to what was described previously—except the resins were at 0% (i.e., the mPRS mixture) and 80% degree of polymerization. To form DGEBA-based mPRS-control and mPRS-modified systems, predetermined amounts of the mPRS resin were added to the blank sample mixtures (i.e., stoichiometric blends of DGEBA and PEDA) to make sample mixtures having 15wt% mPRS resin. In addition, to compare the behavioral characteristics of the resulting DGEBA-based systems with identical TGDDM-based systems having the same mPRS resin inclusion, specified amounts of the mPRS resin were also added to the TGDDM-based blank sample mixtures (i.e., stoichiometric blends of TGDDM and PEDA) to make sample mixtures having 15wt% mPRS resin. All the sample mixtures were well mixed and degassed, and then oven-cured at 80 °C for 24 hours and post-cured at 160 °C for 4 hours. The curing protocol of these mixtures was substantially similar to the one used for sample mixtures made from TGDDM and PEDA, described previously.

Figures 12 and 13 represent the tensile stress-strain behavior of the mPRS-control and the mPRS-modified systems of the DGEBA-based and the TGDDM-based epoxy, respectively. Similar to what was shown previously, the mPRS-modified systems of both the DGEBA-based and the TGDDM-based

epoxies revealed larger elongation-to-failure than their corresponding mPRS-control systems. The graphs further indicate that the improvement of elongation-to-failure of the mPRS-modified systems has been obtained without a considerable drop in Young's modulus and tensile strength. Average values of the Young's modulus, the tensile strength, and the elongation-to-failure were measured from at least four replicates per sample, which are all listed along with the corresponding deviations in Table 2. These results show that the mPRS toughening method has been successfully applied to the DGEBA-based epoxies as well. The results further suggest the mPRS toughening method, as described, is applicable to other thermosetting chemistry that produces a crosslinked network structure.

Comparison of the strain recovery between the mPRS-modified DGEBA-based and the mPRS-modified TGDDM-based epoxy systems. Evidence of strain softening (necking) was observed in the tested specimens of DGEBA-based mPRS-modified epoxy systems, whereas no such evidence was observed in the identical TGDDM-based mPRS-modified epoxy systems. The observed strain softening in the DGEBA-based mPRS-modified epoxy systems, which is also apparent in Figure 12, could be related to the difference in T_g. Shown in Table 2, an average T_g of the DGEBA-based mPRS-modified epoxy systems is about 84 °C, whereas this quantity is approximately 149 °C for the TGDDM-based mPRS-modified epoxy systems. Since the quasi-static test has been performed on both systems at room temperature (i.e., about 25 °C), the difference between the testing temperature and the T_g of each system was higher in the TGDDM-based mPRS-modified systems compared to the DGEBA-based mPRS-modified systems. Such a difference causes higher localized shear deformation in the DGEBA-based system that manifests as strain softening behavior under quasi-static loading.

A strain recovery test was performed to evaluate each of the DGEBA-based and the TGDDM-based mPRS-modified epoxy systems at the same mPRS inclusion (i.e., 15wt%). Accordingly, an mPRS-modified specimen of each DGEBA- and TGDDM-based epoxy system (with 15wt% mPRS inclusion) was loaded to 6.5% strain and subsequently unloaded in a cyclic manner for two cycles and then loaded again until the specimen broke. The 6.5% strain was chosen to ensure the material was strained beyond its elastic limit to undergo a plastic deformation, based upon the stress-strain behavior shown in Figure 12 and 13. The representative stress-strain behavior of each DGEBA-based and TGDDM-based epoxy system subjected to the cyclic tensile loading is shown in Figure 14 and 15.

8 | *J. Mater. Chem. A.*, 2020, **00**, 1-3

This journal is © The Royal Society of Chemistry 2020
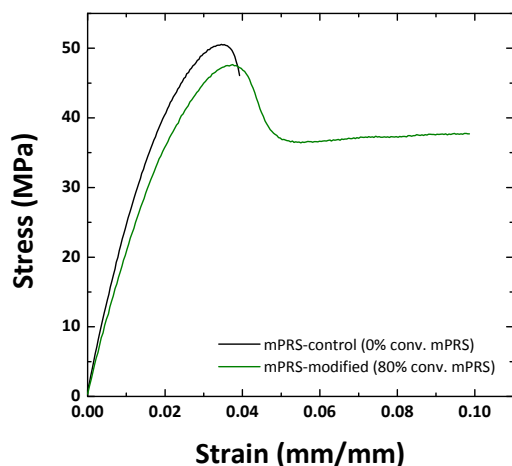
Journal of Materials Chemistry A

Figure 12. Representative tensile stress-strain curves of the DGEBA-based epoxy systems having 15wt% mPRS resin.
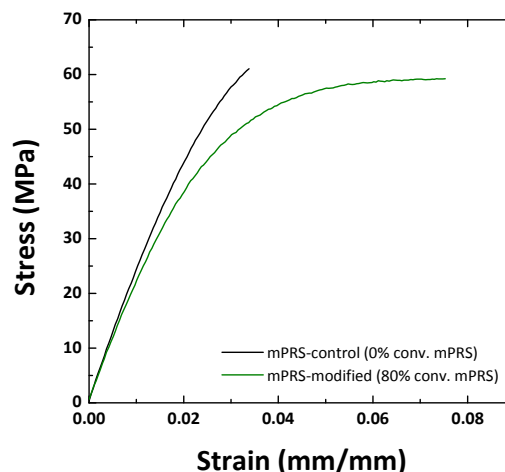

Figure 13. Representative tensile stress-strain curves of the TGDDM-based epoxy systems having 15wt% mPRS resin.

Table 2. Average values of the Young's modulus, tensile strength, and elongation-to-failure of the DGEBA-based and the TGDDM-based epoxy systems.

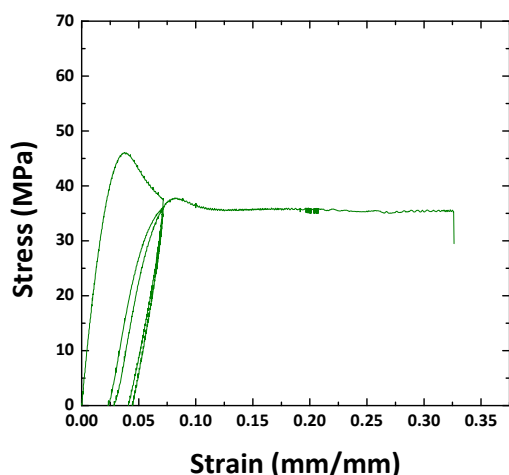|		Young's modulus (GPa)		Tensile strength (MPa)		Elongation-to-failure (%)		Glass transition temp. (°C)	
		mPRS degree of polymerization		mPRS degree of polymerization		mPRS degree of polymerization		mPRS degree of polymerization	
		0%	80%	0%	80%	0%	80%	0%	80%
15% mPRS Content	DGEBA	2.4 ± 0.1	2.0 ± 0.1	49.8 ± 4.3	46.7 ± 1.6	4.0 ± 1.1	9.5 ± 2.2	81	84
	TGDDM	2.4 ± 0.1	2.1 ± 0.1	61.1 ± 3.4	58.9 ± 2.3	3.4 ± 1.3	7.3 ± 2.2	134	149

Figure 14. Representative stress-strain behavior of the DGEBA-based epoxy system having 15wt% mPRS under a cyclic tensile load.
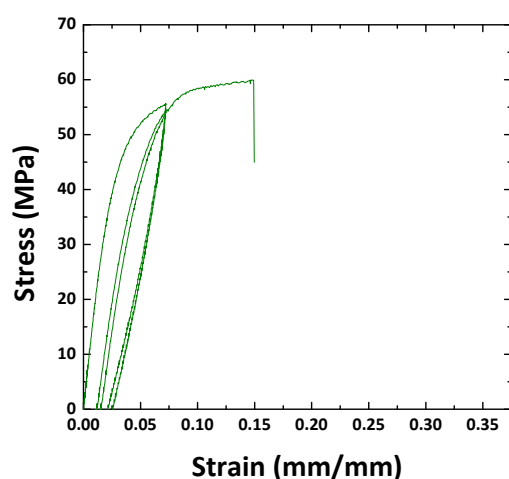

Figure 15. Representative stress-strain behavior of the TGDDM-based epoxy system having 15wt% mPRS under a cyclic tensile load.

A comparison of each system's strain recovery values indicated that straining the DGEBA-based specimen to the 6.5% strain and subsequently unloading the specimen resulted in about a 4.5% permanent strain in the specimen, whereas this quantity is substantially lower (i.e., about 2.5% permanent strain) in the TGDDM-based specimen. The reduced permanent deformation in the TGDDM-based specimen could be due to the difference between the testing temperature and T_g, as described previously. Further, the reduced permanent deformation in the TGDDM-based specimen may also be related to the difference in the crosslinking density of each sample. The TGDDM-based specimen has a higher crosslinking density than that of the DGEBA-based specimen because TGDDM is a tetra-functional epoxy resin, while DGEBA is a di-functional epoxy resin. Such a difference causes a difference in localized shear deformations, with the lower-T_g system (i.e., the DGEBA-based epoxy) having a higher localized shear deformation. The higher localized shear deformation in the lower-T_g system may exhibit in the form of strain softening under quasi-static loading.

.

Interestingly, both systems exhibited larger elongation-to-failure values when subjected to cyclic tensile loading. This was found by comparing the stress strain behavior of the TGDDM-based and DGEBA-based systems under cyclic tensile loading to their behavior under non-cyclic tensile loading. This observation can be explained by the presence of the molecular surfaces (in the form of the mPRS). As described previously, the contribution of microvoid growth to the total absorbed energy is considerable in the mPRS-modified systems. Under noncyclic tensile loading (Figure 12 and 13), an applied stress may deform only a portion of the total mPRS present in the system, whereas when under cyclic tensile loading, the preloading of the system to a strain value beyond the elastic limit may contribute a greater number of the mPRS regions to the total energy absorbed by the system without bond breaking. Therefore, both the mPRS-modified TGDDM-based and the DGEBA-based system produce an enhanced elongation-to-failure when loaded in a cyclic manner. In view of this the mPRS-modified systems are believed to be good candidates to replace epoxies currently used for composite manufacturing.

Processing advantages of using mPRS resins. One important aspect of toughening epoxy systems using partially reacted substructures, as described in this study and our previous study,[37] is the viscosity of the mPRS resin additive and its shelf life. To be largely applicable to industrial settings, the mPRS resins must have low viscosity and low reactivity at the processing conditions, particularly when the mPRS resin is present at an elevated degree of polymerization close enough to the gelation point. In addition, the mPRS resin should have good miscibility with the epoxy resin and the curing agent.

The PRS resin used in our previous study[37] offered unique thermal and mechanical characteristics compared to the solvent-modified systems, however, scaling-up the processes to use the PRS-modified systems (e.g., in composite manufacturing via VARTM for example) may be challenging. The viscosity of PRS-resins increases as the degree of polymerization rises, particularly when the degree of polymerization of a PRS resin is close to the gelation point. The mPRS-resin used in this study, however, overcomes this challenge and is therefore a good replacement for the PRS resin that was previously used. A rheology test on an 80%-conversion PRS resin of our previous study[37] and an 80%-conversion mPRS resin of the current study revealed that at the same temperature, the viscosity of the mPRS resin is about five times lower than that of the PRS resin. This is very advantageous from a manufacturing perspective, as a lower resin viscosity significantly facilitates the resin transfer operations.

In addition to the viscosity, the additive should have a prolonged shelf life for large scale manufacturing. The mPRS is more advantageous in this respect because it is less reactive than the PRS resin of our previous study[37] due to the absence of one amine in the curing agent molecules. Furthermore, the polyethylene glycol backbone of the PEMA molecules makes the mPRS resin crystallizable at room temperature. As a result, curing reactions are extremely suppressed within the mPRS resin when it is at a crystallized state, and thus the shelf life of the resin is prolonged significantly, without changing the resin's degree of polymerization over time.

10 | *J. Mater. Chem. A.*, 2020, **00**, 1-3

This journal is © The Royal Society of Chemistry 2020

Conclusion

A method of toughening amine-cured epoxy systems was developed, and the resulting epoxy systems were characterized. According to the method, a monoamine-functionalized Partially Reacted Substructures (mPRS) resin was produced by partially curing a mixture of tetraglycidyl ether of diaminodiphenylmethane (TGDDM) and polyether monoamine (PEMA). A predetermined amount of the mPRS resin having 0%, 60%, and 80% degree of polymerization was further added to a pre-cured mixture of a TGDDM-based epoxy system and a DGEBA-based epoxy system, and the mixtures were cured. Results of the quasi-static tensile test on the cured samples revealed a large strain hardening and, subsequently, a large elongation-to-failure in the mPRS-modified systems having mPRS resins at elevated degrees of polymerization. The improved elongation-to-failure was found to be due to an enhanced plastic microvoid growth as a result of the presence of the mPRS regions (i.e., molecular surfaces) within the crosslinked structure of the mPRS-modified epoxy systems. These molecular surfaces appeared as microvoids in the micrographs of the fracture surfaces. It was also shown that the mPRS-modified systems have higher fracture toughness values and slightly higher glass transition temperatures than the corresponding mPRS-control systems. The observed improvement in ductility, toughness, and glass transition temperature of the mPRS-modified systems was obtained without a considerable drop in Young's modulus and tensile strength of the epoxy systems. Finally, it was shown that the proposed method of toughening is applicable to other thermosetting systems that form a crosslinked network structure.

Acknowledgements

Notes and references

1. R. A. Pearson and A. F. Yee, *Journal of Materials Science*, 1991, **26**, 3828-3844.
2. R. Bagheri, B. T. Marouf and R. A. Pearson, *Polym. Rev.*, 2009, **49**, 201-225.
3. R. Bagheri and R. A. Pearson, *Polymer*, 1996, **37**, 4529-4538.
4. A. Labak and R. A. Pearson, *Proc. Annu. Meet. Adhes. Soc.*, 2014, **37th**, 1-3.
5. R. M. Hydro and R. A. Pearson, *J. Polym. Sci., Part B: Polym. Phys.*, 2007, **45**, 1470-1481.
6. H. Kishi, Y. Kunimitsu, J. Imade, S. Oshita, Y. Morishita and M. Asada, *Polymer*, 2011, **52**, 760-768.
7. X. Yang, F. Yi, Z. Xin and S. Zheng, *Polymer*, 2009, **50**, 4089-4100.
8. K. H. Hsieh and J. L. Han, *J. Polym. Sci., Part B: Polym. Phys.*, 1990, **28**, 783-794.
9. M.-S. Lin, C.-C. Liu and C.-T. Lee, *J. Appl. Polym. Sci.*, 1999, **72**, 585-592.
10. T. Iijima, T. Horiba and M. Tomoi, *Eur. Polym. J.*, 1991, **27**, 1231-1238.
11. Z. G. Shaker, R. M. Browne, H. A. Stretz, P. E. Cassidy and M. T. Blanda, *J. Appl. Polym. Sci.*, 2002, **84**, 2283-2286.
12. S. Sprenger, *Polymer*, 2013, **54**, 4790-4797.
13. G. Di Pasquale, O. Motta, A. Recca, J. T. Carter, P. T. McGrail and D. Acierno, *Polymer*, 1997, **38**, 4345-4348.
14. A. J. Kinloch, M. L. Yuen and S. D. Jenkins, *J. Mater. Sci.*, 1994, **29**, 3781-3790.
15. R. J. Day, P. A. Lovell and D. Pierre, *Polym. Int.*, 1997, **44**, 288-299.
16. US5464902A, 1995.
17. R. Bagheri and R. A. Pearson, *J. Mater. Sci.*, 1996, **31**, 3945-3954.
18. R. Bagheri and R. A. Pearson, *Polymer*, 1999, **41**, 269-276.
19. J. Y. Qian, R. A. Pearson, V. L. Dimonie and M. S. El-Aasser, *J. Appl. Polym. Sci.*, 1995, **58**, 439-448.
20. CN102190858A, 2011.
21. J. Gao, J. Li, S. Zhao, B. C. Benicewicz, H. Hillborg and L. S. Schadler, *Polymer*, 2013, **54**, 3961-3973.
22. P. Rosso, L. Ye, K. Friedrich and S. Sprenger, *J. Appl. Polym. Sci.*, 2006, **100**, 1849-1855.
23. B. Zewde, P. Pitliya and D. Raghavan, *J. Mater. Sci.*, 2016, **301**, 542-548.
24. B. Boesl, B. V. Sankar and W. G. Sawyer, *Proc. Am. Soc. Compos., Tech. Conf.*, 2006, **21st**, 145/141-145/147.
25. S. Julyes Jaisingh, V. Selvam, M. Suresh Chandra Kumar and K. Thyagarajan, *Adv. Mater. Res.*, 2013, **651**, 154-158, 156 pp.
26. D. Haba, A. J. Brunner and G. Pinter, *Compos. Sci. Technol.*, 2015, **119**, 55-61.
27. B. Wetzel, P. Rosso, F. Haupert and K. Friedrich, *Engineering Fracture Mechanics*, 2006, **73**, 2375-2398.
28. Y. T. Park, Y. Qian, C. Chan, T. Suh, M. G. Nejhad, C. W. Macosko and A. Stein, *Advanced Functional Materials*, 2014.
29. F. H. Gojny, M. H. G. Wichmann, B. Fiedler and K. Schulte, *Composites Science and Technology*, 2005, **65**, 2300-2313.
30. M. A. Rafiee, F. Yavari, J. Rafiee and N. Koratkar, *Journal of Nanoparticle Research*, 2011, **13**, 733-737.
31. N. Wang, Y. Shao, Z. Shi, J. Zhang and H. Li, *J. Mater. Sci.*, 2008, **43**, 3683-3688.
32. Z. Zhang, G. Liang, C. Fang and J. Pei, *Jueyuan Cailiao*, 2012, **45**, 40-42, 46.
33. D. Mukherji and C. F. Abrams, *Physical Review E*, 2008, **78**, 050801.
34. D. Mukherji and C. F. Abrams, *Physical Review E*, 2009, **79**, 061802.
35. M. Sharifi, C. W. Jang, C. F. Abrams and G. R. Palmese, *J Mater Chem A*, 2014, **2**, 16071-16082.

This journal is © The Royal Society of Chemistry 2020

J. Mater. Chem. A., 2020, **00**, 1-3 | **11**

36.   C. Jang, M. Sharifi, G. R. Palmese and C. F. Abrams, *Polymer*, 2014, **55**, 3859-3868.
37.   M. Sharifi, C. Jang, C. F. Abrams and G. R. Palmese, *Macromolecules,* 2015, **48**, 7495-7502.
38.   J. Mijovic and S. Andjelic, *Macromolecules*, 1995, **28**, 2787-2796.
39.   V. I. Raman and G. R. Palmese, *Macromolecules*, 2005, **38**, 6923-6930.
40.   C. Jang, M. Sharifi, G. R. Palmese and C. F. Abrams, *Polymer*, 2016, **90**, 249-255.
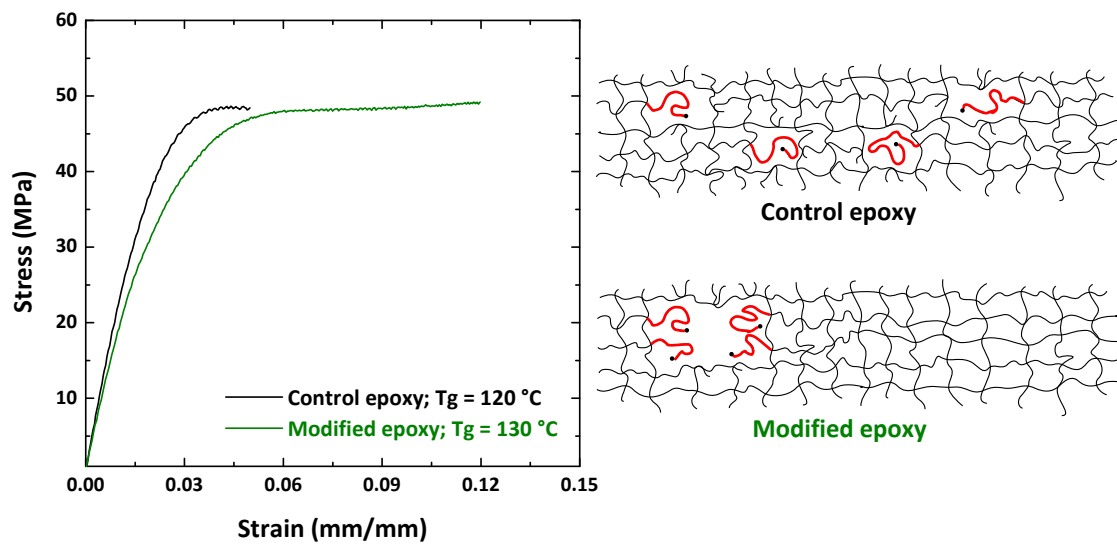
TOC: Ductile high-T_g epoxy systems via a controlled dispersion of mono-functional components